EPJ Web of Conferences **26**, 01034 (2012)
DOI: 10.1051/epjconf/20122601034

Laser-driven plasma loader and solid matter ramp compression experiments on SG-II Laser

M. Li[1], X. Huang[2], G. Chen[1], J. Cai[1], H. Zhang[1], C. Sun[1,2], J. Zhao[1], S. Liu[1], and S. Fu[2]

[1] *Institute of Fluid Physics, PO Box 919-113, Mianyang, Sichuan 621900, China*
[2] *Shanghai Institute of Laser Plasma, PO Box 800-229, Shanghai 201800, China*

Abstract. Laser-driven plasma loader for shockless compression provides a new approach to study the rapid compression response of materials. But little information about the "plasma piston" can be obtained. The objective of the current study tried to map out a whole procedure of laser-driven plasma jet and shockless compression of solid materials. The experiment was performed using the Shenguang-II Nd: glass laser. Shock wave transmitting in reservoir, and Al/LiF interface velocity history both are recorded by a 2-channel line VISAR. Streaked and separated shade graph of plasma jet from rear surface of reservoir gave the 2D configuration and front speed (about 28 km/s to 60 km/s). A coaxial M-Z interferometer system is used for plasma density diagnostic. The density distribution is downward bulge near front of plasma jet, which is an important characteristic that determines shockless compression. Shockless compression of 30/40μ m Al step backed by 1mm LiF presented smooth pressure history up to 20GPa. The strain rate can reach $10^{7\sim8}$/s.

1 Introduction

Laser-driven plasma loader for shockless compression provides a new approach to study the rapid compression response of materials [1–7]. Currently, this method is utilized widely, including in EOS (Equation of state), phase transformation at high pressure, and strength of material. Many experiments have presented similar results, wherein only the particle velocity of the compressed sample was measured directly. However, no dynamic data of the "plasma piston" are provided [6]. Thus, little information about the "plasma piston" can be obtained, which is the driving source of the sample compression, and is very important for understanding and the application of the shockless loading method. As laser radiating on reservoir film, there exist complex response in reservoir. Figure 1(L) shows two typical simulation results of the simulated density contours (x-t graph) of the laser-driven reservoir and its interaction with compression target. AB is the critical surface during laser irradiation, and AE is the shock front, AL is the front of the ablated plasma jet, BC is the head of the leftward compression wave, and BD is the head of the rightward rarefaction waves. If the unloading wave captures the shockwave at Point D, Then, the shock strength attenuates, as evidenced by the decreasing density. when the shock reach rear surface of reservoir, a plasma jet formed with a speed higher than 3 times of initial particle velocity post shock. Figure 1(R) is an x-t graph of the density contours near the drive surface. Five zones with different characteristics can be found: the free plasma jet, the stagnating plasma, the melted zone, the compressed sample, and the uncompressed sample. The figure shows that the compression wave spreading into the sample changes from a ramp wave into a shockwave. The distance in which the compression is shockless suggests the maximum sample thickness. The spread velocity of the stagnated shock in the plasma jet evidently increases when the total pressure of the jet before the stationary shock starts to drop. Then, the drive pressure begins to decline. These are main procedure of laser-driven plasma jet and shockless compression of solid materials, in this paper, we tried to show these in experiments.

2 Experimental setup

The experiment was performed using the Shenguang-II Nd: glass laser (converted at $\lambda = 527$ nm, or 351nm) of the National Laboratory on High Power Laser and Physics. The temporal profile of the laser is nearly square with a rise and fall time of ~300 ps and a full width at half maximum of ~3 ns. A lens array (LA) was used to eliminate the large scale spatial modulation and to obtain a flat-topped profile in the focal plane. The characteristics of the optical system (lens+LA) were such that the focal spot had a $\sim 1.2 \times 0.8$ mm (for 2ω) hexagon or a 2.0×1.5 mm(for 3ω) rectangle flat region. The experiment setup is shown in Figure 2. A coaxial M-Z interferometer system coupled with shade graph recorder is used for plasma jet diagnostic. A 2-channel line VISAR is used for measurement of shock velocity in reservoir or ramp wave in compression sample. The reservoir material is 200 μm polystyrene (C8H8)(for 1.2×0.8 mm spot), or 125 μm polyimide(for 2.0×1.5 mm spot), covered with 200nm Al foil at the ablation surface as shield of incident drive laser.

The vacuum is a 280 μm thick spacer and Al samples were either a 30/40 μm thick stepped foil attached to a LiF window. For Al/LiF samples, Al was coated directly onto stepped LiF windows with electron-beam deposition at a growth temperature of ~ 450 K. After deposition, the Al surface away from the mandrel was diamond turned to achieve planarity. Bragg diffraction showed a preferential [111] fcc structure in the growth direction. Samples were measured to be fully dense (2.69g/cc) to within an accuracy of 1%. The source Al was 99.999% pure. White-light interferometry was used to ensure a surface roughness, thickness gradients and step heights. The high purity LiF was orientated with the [100] axis along the pressure

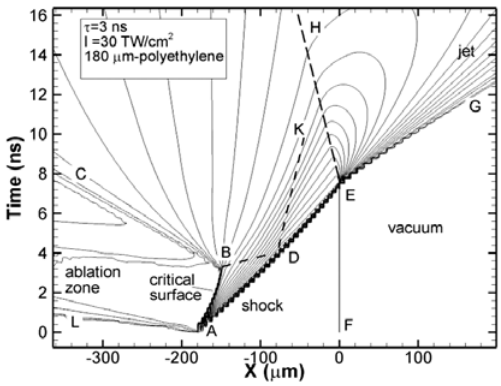

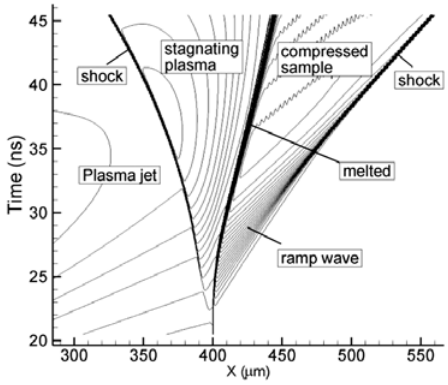

Fig. 1. Simulation results of laser driven plasma loader and ramp compression.

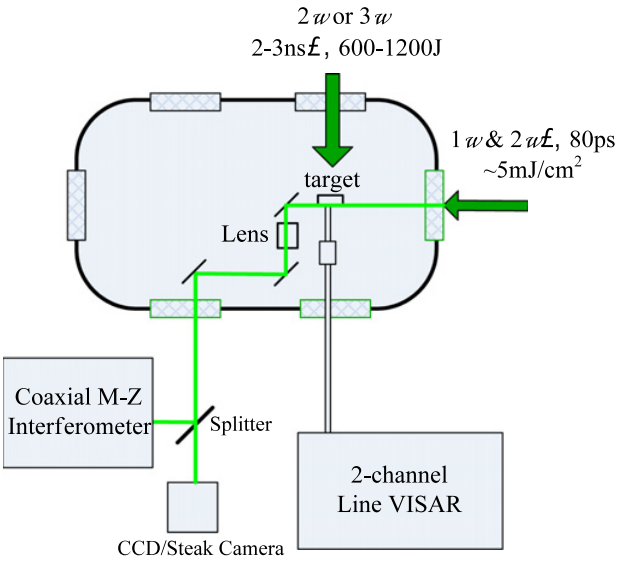

Fig. 2. Schematic of Experimental setup.

loading direction. As the particle-velocity wave reaches the back surface of the Al, it begins to accelerate into the LiF window. The interface-velocity history is recorded with a line-imaging velocity interferometer (VISAR) with two channels set at different sensitivities.

With velocity history of window interface, backward integration method is used to calculate the in situ particle velocity and loading history inside the sample. Here the

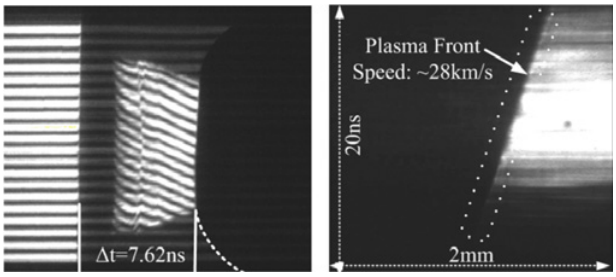

Fig. 3. (a) Shock wave transmit in reservoir (5 km/s/fringe), (b) streaked shade graph of plasma jet from rear surface of reservoir. Drive laser: 527 nm, 3 ns, 818 J, and laser spot 1.2 × 0.8 mm.

rate-dependent Steinberg constitutive model is combined for calculation the stress deviator and Hydrostatic pressure of solid matter.

3 Results and discussion

3.1 shockwave in the reservoir and jet formation

When laser radiating on reservoir surface, there is an incident shock propagating into reservoir, but at first, a Marshark wave is formed ahead shock wave, this wave makes part of reservoir ionized ahead of shock, thus can be seen in Fig. 3 (a), shock front reflection signal occurs several ns after laser time. And there exist a jump of shock velocity because of "M" laser profile. The second peak produced another shock which runs faster than the first on and catch it at the time of jump. Then shock wave speed in reservoir decreases more than 10 km/s, and the total breakout time is 7.62 ns. The total average speed is 26.2 km/s, the plasma jet formed from the rear surface of reservoir, and its front speed is about 28 km/s here. Also it can be seen that the jet velocity changes little after its formation. In another experiments using higher laser intensity, the front speed can be higher than 60 km/s.

3.2 Characteristic of laser direct-drive plasma loader

As the plasma jet goes forward, its density gradient behind front decrease smoothly under the effect of rarefaction waves. Meanwhile, the rarefaction waves from side also changes the jet to a mushroom. Figure 4 presents the 2D configuration of side view. If amplify the front zone, there can be seen smooth fringe phase shift, that means the jet front is very rarefied and there is no density jump. The 3D figure shows the density distribution near the jet front. And the density profile bulges downward near the jet front, which is an important characteristic that determines shockless compression.

When the laser spot changes to 2 mm, the side rarefaction can be controlled to a relative small zone, and there is still large range of jet can be treated as 1D flow. Figure 5 shows the result of 2 mm laser spot with both 1ω & 2ω probe laser. In the figure, we can see the flat range is more than 1mm, and its enough to do double-step target. Figure 5(R) give out the phase shift near the jet front for

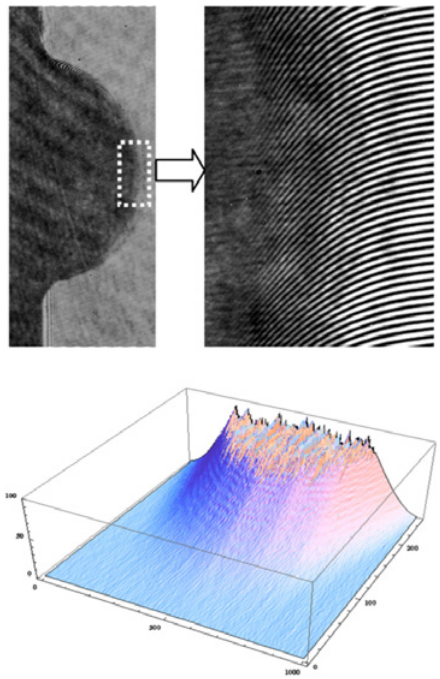

Fig. 4. 2D configuration and density distribution of the plasma piston. E(2ω) = 726 J, laser spot 1.2 × 0.8 mm.

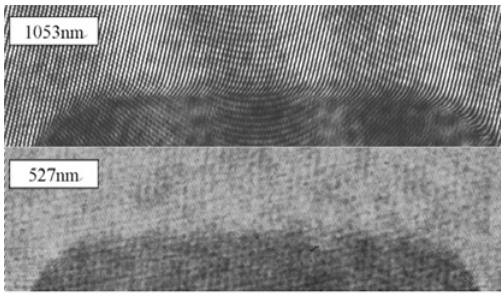

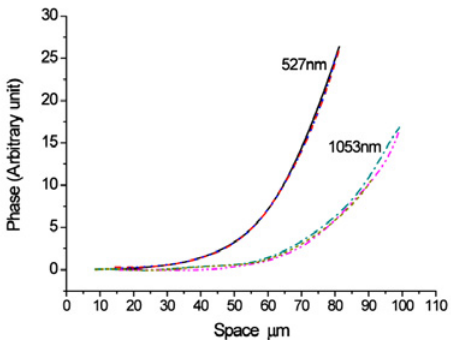

Fig. 5. 2D interfering picture with both 1ω &2ω probe laser (L), phase shift distribution of the plasma front. E(3ω) = 1000 J, laser spot 2.0 × 1.5 mm.

double probe wavelength. It shows that the phase shift is an inverse relation to wave length, which means the ionization degree is very poor and approach to zero.

3.3 Ramp compression of solid matter

If place an Al/LiF target downstream the reservoir jet, the jet will impact on the target and the target will be

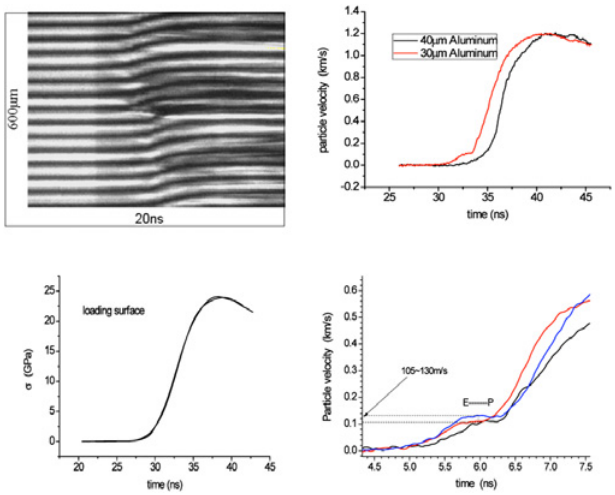

Fig. 6. (a) A typical VISAR record reflected from the rear of a 30/40 μm Al step backed by 1.5 mm LiF. (b) Particle velocity history of each step, (c) Drive pressure history of Aluminum loading surface according to backward integration. (d) Elastic plastic behavior of monocrystalline Aluminum, under high rate (2.0×10^7/s) ramp compression.

compressed smoothly because of the smooth jet front. Figure 6 (a) presents a typical VISAR result of a 30/40 μm Aluminum step. Fringe motion indicates acceleration of the surface (1.612 km/s/fringe). The particle velocity history is given in Fig. 6(b) after correction according to LiF refractive rate. Then the backward integration method coupled with rate-dependent Steinberg constitutive model is utilized to calculation the mechanic response inside Aluminum sample. Figure 6(c) shows the pressure history at the loading surface. From the figure, it can be seen that the loading history calculated from both step agrees very well, and rise smoothly to 23 GPa from normal condition. There is another characteristic for all shots, the velocity history has a shoulder in the range 105 m/s to 130 m/s, as shown in Fig. 6(d). It is interpreted as elastic-plastic transition [7]. In this article, the peak shockless pressure is about 20 GPa to 25GPa, and the coherent peak strain rate is about 2.0×10^7/s. Stress value on the shoulder means the isentropic elastic limit is ~1.4 GPa.

Acknowledgements

The authors would like to thank the SG-Laboratory for the support it has provided for this work. We also would like to thank Dr. R. F. smith for his helpful suggestions. This work was supported by the Natural Science Foundation of China (No.11172280) and Foundation of CAEP (No.2011B0201004).

References

1. J. Edwards, K. T. Lorenz, B. A. Remington, et al., Phys. Rev. Lett. 92(7), 075002, (2004).

2. K. T. Lorenz, R. F. Smith, S. G. Glendinning, et al., Phys. Plasmas 12, 056309, (2005).
3. R. F. Smith, J. H. Eggert, A. Jankowski, et al, Phys. Rev. Lett. 98, 065701, (2007).
4. R. F. Smith, S. M. Pollaine, S. J. Moon, et al., Phys. Plasmas 14, 057105, (2007).
5. E. I. Moses, R. N. Boyd, B. A. Remington, et al., Phys. Plasma 16:041006, (2009).
6. M. Li, H. Zhang, C. Sun, et al., J. Appl. Phys., 109, 093525 (2011).
7. R. F. Smith, J. H. Eggert, R. E. Rudd, et al., J. Appl. Phys., 110, 123515 (2011).